J Mol Med
DOI 10.1007/s00109-017-1555-z

JMolMed

ORIGINAL ARTICLE

# Cathelicidin-deficient mice exhibit increased survival and upregulation of key inflammatory response genes following cecal ligation and puncture

**Patricia Severino[1] · Suely Kubo Ariga[2] · Hermes Vieira Barbeiro[2] · Thais Martins de Lima[2] · Elisangela de Paula Silva[1] · Denise Frediani Barbeiro[2] · Marcel Cerqueira César Machado[2] · Victor Nizet[3,4] · Fabiano Pinheiro da Silva[2,5]**

Received: 6 January 2017 / Revised: 15 May 2017 / Accepted: 31 May 2017


**Abstract**
Antimicrobial peptides possess a myriad of molecular properties including bacterial killing and the regulation of many aspects of innate immunity. Cathelicidins are a group of antimicrobial peptides widely investigated by the scientific community. Many studies have focused on the bactericidal and pro-inflammatory roles of cathelicidins. Because the role of endogenous cathelicidin expression remains obscure in deep-seated systemic infections, we induced sepsis in cathelicidin knockout and wild-type (WT) mice by cecal ligation and puncture, performing transcriptome screening by DNA microarray in conjunction with other immunologic assays. Cathelicidin-deficient mice showed increased survival compared to WT mice in this established experimental model of polymicrobial sepsis, in association with upregulation of certain key inflammatory response genes. Therefore, cathelicidins can exert both pro- and anti-inflammatory activities depending on the disease and cellular context.

**Key messages**
- The role of cathelicidin in a CLP model is investigated using cathelicidin-KO mice.
- Cathelicidin-KO mice show an enhanced immune response and improved survival rates.
- An anti-inflammatory effect of cathelicidin is likely to be detrimental for CLP.
- Cathelicidin-KO mice show upregulation of genes associated with increased plasma levels of pro-inflammatory Ils.
- Cathelicidins appear to have both pro- and anti-inflammatory properties.

**Keywords** Sepsis · Cathelicidin · Inflammation · Gene expression

## Introduction

Cathelicidins are antimicrobial peptides (AMPs) that possess critical roles in mammalian innate immune defense against invasive bacteria, viruses, and fungal infection. Cathelicidin-related peptides are highly heterogeneous but are characterized by a conserved region (cathelin domain) [1].

While some mammals express multiple cathelicidins, just a single member of this AMP family is found in humans and mice [2]. Human cathelicidin (LL-37) and murine cathelicidin (CRAMP) closely resemble one another in size, architecture of encoding genes, proteolytic processing from inactive precursor to mature peptide, amphipathic α-helical structure, overall cationic charge, tissue and cellular distribution of expression, and spectrum and mechanism of antimicrobial activity [3].

**Electronic supplementary material** The online version of this article (doi: 10.1007/s00109-017-1555-z) contains supplementary material, which is available to authorized users.

✉ Fabiano Pinheiro da Silva
pinheirofabiano@hotmail.com

[1] Instituto Israelita de Ensino e Pesquisa, Hospital Israelita Albert Einstein, São Paulo, Brazil

[2] Departamento de Emergências Clínicas, Faculdade de Medicina da Universidade de São Paulo, São Paulo, Brazil

[3] Division of Host-Microbe Systems and Therapeutics, Department of Pediatrics, UC San Diego, La Jolla, CA, USA

[4] Skaggs School of Pharmacy and Pharmaceutical Sciences, UC San Diego, La Jolla, CA, USA

[5] Faculdade de Medicina da Universidade de São Paulo, Laboratório de Emergências Clínicas (LIM-51), Av. Dr. Arnaldo, 455 sala 3189, São Paulo, São Paulo CEP 01246-000, Brazil

Published online: 16 June 2017

Cathelicidins were originally identified in neutrophils [4, 5] but have since been found in many other immune and epithelial cell types including macrophages and keratinocytes [6, 7].

A study of bacterial skin infection in CRAMP-deficient mice was the first to demonstrate an essential role for an AMP in mammalian innate immunity [7], and further investigations in this model have shown that cathelicidin contributes to antibacterial defense of the gastrointestinal tract [8], urinary tract [9], and ocular mucosa [10].

Like many AMPs, the bactericidal activities of cathelicidins are related to their cationic nature, which promotes interactions with and the destabilization of anionic bacterial cell walls and membranes [11]. Cathelicidins bind to lipopolysaccharide (LPS) [12, 13] and other pathogen-associated patterns [14], activate membrane receptors [15–17], induce chemotaxis [18, 19], trigger the inflammasome [20], induce apoptosis and other mechanisms of cell death [21, 22], among other immunoregulatory and non-immune functions [6].

A recent study from our group demonstrated that LL-37, the human cathelicidin, is downregulated in neutrophils from patients in septic shock when compared with severe sepsis or patients recovering from septic shock [23]. Others have shown that LL-37 plasma levels were downregulated when patients with sepsis were compared with healthy controls [24]. To contribute to the current understanding of the role of cathelicidin in severe systemic infection, we induced sepsis in cathelicidin-deficient mice, using the cecal ligation and puncture (CLP) model, and compared their mortality to wild-type controls. In this infection model, survival rates for septic cathelicidin-deficient mice were significantly higher when compared with those for control mice. Gene expression profiling identified that important immune response genes and neutrophil infiltration to the site of infection were significantly upregulated in cathelicidin-deficient mice.

## Materials and methods

### Mice

CRAMP$^{-/-}$ mice in the C57BL/6 genetic background [7] and their matched wild-type (WT) controls were purchased from The Jackson Laboratory (ME, USA). All experiments were performed when animals were 8–12 weeks old and protocols followed in accordance with the University of São Paulo Faculty of Medicine Animal Facility guidelines through protocols approved by their ethics committee.

### Mouse model for sepsis using cecal ligation and puncture

We induced peritonitis in mice using the model of CLP as previously described [25]. Briefly, the cecum was perforated allowing the release of fecal material into the peritoneal cavity, eventually leading to systemic infection. Animals were anesthetized and the cecum ligated and punctured twice with a 21G needle. To obtain a mortality curve, 12 mice from each group underwent CLP. Mice were observed every 12 h until death or euthanasia by day 5. Data from two independent experiments are presented with a total number of 24 animals per group.

### RNA extraction and microarray experiments

Blood from eight CRAMP-deficient mice and eight WT mice was collected by cardiac puncture and stored in RNAlater (Ambion, USA), 8 h after CLP. Total RNA was isolated using a Mouse RiboPure-Blood kit following the manufacturer's protocol (Ambion, Thermo Fisher, USA). RNA integrity and concentration were assessed using the Agilent 2100 Bioanalyzer and the RNA 6000 Nano Kit (Agilent Technologies, USA). Expression levels were evaluated using the SurePrint G3 8x60K Mouse Gene Expression v2 Microarray (design ID G4858A-074809) and the Low Input Quick Amp Labeling kit, following a one-color labeling protocol (Agilent Technologies, USA). This mouse gene expression microarray version covers the complete set of RefSeq coding transcripts (NM) from the latest build as well as updated long non-coding RNA (lncRNA) content (27,122 unique Entrez Genes and 4578 unique lncRNAs).

### Microarray data processing and analysis

Microarrays were scanned using the SureScan Microarray Scanner (Agilent Technologies) and images processed using the Feature Extraction Software v12 (Agilent Technologies) for quality control, determination of feature intensities, and background correction. GeneSpring (Agilent Technologies, USA) was used for data normalization, transformation, and subsequent statistical analysis. Moderated *t* test and one-way ANOVA followed by the Benjamini-Hochberg False Discovery Rate (FDR) correction of *p* values were used for the identification of differentially expressed genes between CRAMP-deficient, WT, healthy, and septic animals. Principal component analysis (PCA) was used for global gene expression analysis, and biological functions associated with gene expression patterns explored using Gene Ontology (GO) term enrichment analysis and KEGG pathway mapping through DAVID Bioinformatics Resources 6.7 (http://david.abcc.ncifcrf.gov). Differentially expressed genes are represented in terms of fold-change (FC). The expression data are deposited at the Gene Expression Omnibus (accession number GSE90727).

### Relative quantification of gene expression levels using real-time PCR

To validate microarray gene expression results for CD14, we used relative quantification by real-time PCR. Briefly, 1 μg of total RNA was subjected to reverse transcription using the High-Capacity cDNA Reverse Transcription Kit (Thermo Fisher Scientific, USA) following the manufacturer's protocol. Specific primer pairs (Invitrogen, Thermo Fisher Scientific, USA) were used for the detection of *Cd14* (F:5′ CTGAAGCCTTTCTCGGAGCC3′, R:5′AGCAACAG CAACAAGCCAAG3′) and *Hprt* (F:5′GCCGAGGA TTTGGAAAAAGTG3′, R:5′TGGCCTCCCATCTC CTTCAT3′) gene expression. Final reactions contained 200 nM of primers and followed the manufacturer's protocol for the PowerUp™ SYBR® Green Master Mix (Thermo Fisher Scientific, USA). PCR was carried out in a QuantStudio 6 Flex Real-Time PCR system (Thermo Fisher Scientific) following the fast cycling protocol. Specificity was determined by the detection of a single melt curve and the comparative ΔΔCt method was used for expression analysis [26]. Three biological replicates of each experiment were included in this assay and the real-time PCR run in triplicate for each experiment.

### Plasma cytokines

TNFα, IL-1β, IL-6, IL-10, and MCP-1 plasma levels were measured in CRAMP-deficient mice and WT mice, both healthy and following CLP, using the magnetic bead immunoassay Milliplex® and the MAGPIX® System (Merck Millipore, USA).

### Phagocytosis assay

Healthy CRAMP-deficient and WT mice were euthanized by $CO_2$ inhalation and peritoneal lavage performed using 6 mL of RPMI medium. Peritoneal lavage fluid was then centrifuged at 5000 rpm for 10 min and total cell counts (mainly macrophages) determined. *Escherichia coli* K-12 was labeled with pHrodo Red dye® (Thermo Fisher Scientific, USA), according to the manufacturer's protocol. For phagocytosis quantification, $1 \times 10^5$ cells were incubated with fluorescent bacteria (1:100) for 2 h at 37 °C, in a total volume of 100 μL. Samples were analyzed by flow cytometry using an EasyCyte 8HT® flow cytometer (Guava, Hayward, CA). Phagocytosis was determined based on the fluorescence intensity of cells using the appropriate fluorescence channel. Analyses were performed using Software Express Pro® Guava for a minimum of 10,000 gated events.

### Measurement of peritoneal cell number

To evaluate neutrophil recruitment to the peritoneal cavity, we counted the total number of cells in the peritoneal cavity 24 h after CLP. Briefly, mice were euthanized by $CO_2$ inhalation and peritoneal lavage performed by injection of 1 mL of RPMI medium. Cells were counted on a hemocytometer and trypan blue staining used to confirm cell viability.

### Apoptosis

The appearance of phosphatidylserine (PS) residues (normally hidden within the plasma membrane) on the surface of the cell is an early event in apoptosis and can be used to detect and measure apoptosis. During apoptosis, PS is translocated from the cytoplasmic face of the plasma membrane to the cell surface. Annexin V has a strong, $Ca^{2+}$-dependent affinity for PS and therefore can be used as a probe for detecting apoptosis. Briefly, peritoneal cells were collected ($1–5 \times 10^5$ cells by centrifugation) 24 h after CLP and resuspended in 500 μL of 1× binding buffer. Then, 5 μL of annexin V-FITC and 5 μL of propidium iodide were added and results analyzed by flow cytometry, using FITC signal detector and PI staining by the phycoerythrin emission signal detector. Double-positive (annexin V + propidium iodide) cells were considered necrotic. Double-negative cells were considered to be live cells.

### Statistical analysis

Continuous variables were analyzed by using Student's *t* test or analysis of variance (ANOVA), as appropriate. Post hoc analysis was performed using the Mann-Whitney *U* test. Results are reported as the mean ± standard deviation. A $p$ value $\leq 0.05$ was considered statistically significant.

## Results

A mortality curve through 5 days indicated that CRAMP-deficient mice were more resistant to CLP (83% survival) compared to WT mice (17% survival) (Fig. 1).

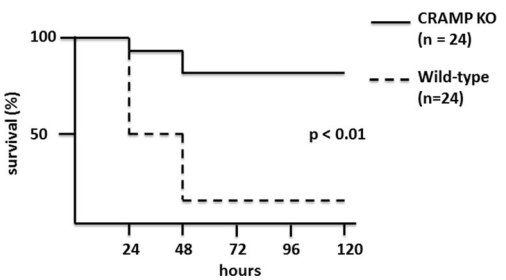


**Fig. 1** Survival curves for septic CRAMP-deficient mice ($n$ = 24) and septic WT mice ($n$ = 24) with CLP. CRAMP-deficient mice exhibited significantly decreased survival compared with WT mice ($p < 0.01$)

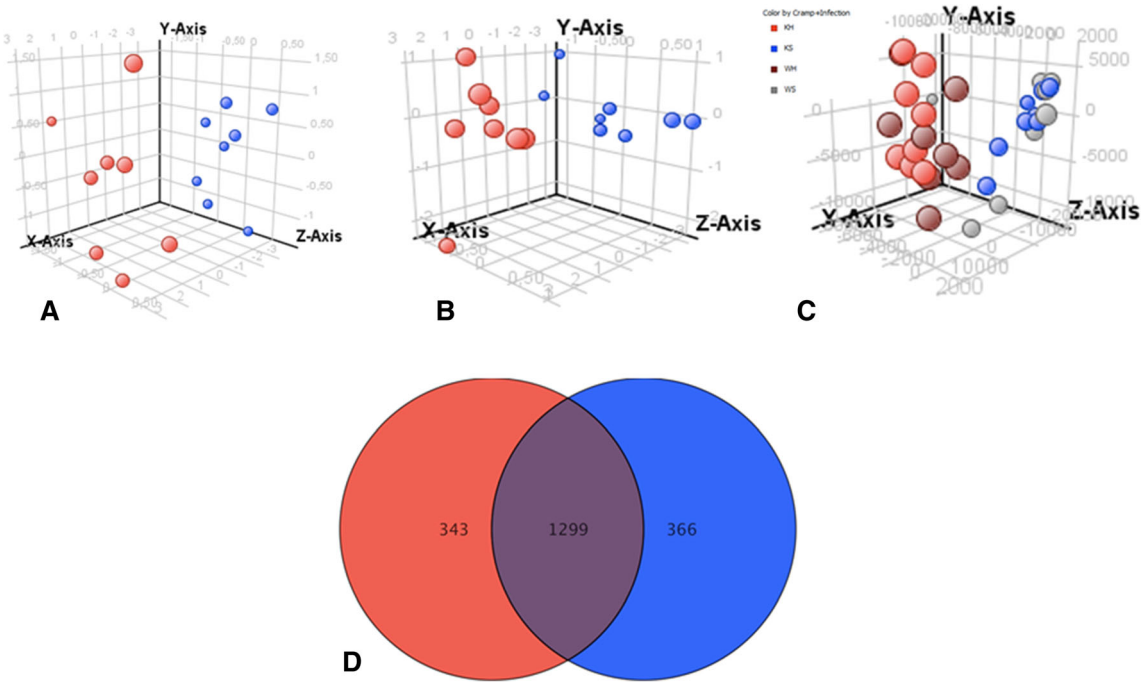


**Fig. 2** **a** Principal component analysis depicting global gene expression profiles of healthy CRAMP-deficient and healthy WT mice samples. *Blue dots* represent CRAMP-deficient mice and *red dots* represent WT mice. The first principal component (*x*-axis) accounts for 83.75% of the variability in the data. **b** Principal component analysis depicting global gene expression profiles of septic CRAMP-deficient and septic WT mice samples. *Blue dots* represent CRAMP-deficient mice and *red dots* represent WT mice. The first principal component (*x*-axis) accounts for 85.65% of the variability in the data. **c** Principal component analysis depicting global gene expression profiles of all CRAMP-deficient and WT animals. *KH* CRAMP-deficient healthy animals (*red dots*), *KS* CRAMP-deficient septic animals (*blue dots*), *WH* WT healthy animals (*dark red*), *WS* WT septic animals (*gray dots*). **d** Venn diagram illustrating the differences and similarities in gene expression between septic CRAMP-deficient mice vs. healthy CRAMP-deficient mice (1642 transcripts) and septic WT mice vs. healthy WT mice (1665 transcripts). A total of 1299 transcripts were similarly regulated in the two groups. Selected genes for this analysis had an FC >2 and FDR-corrected *p* value <0.05

We used global gene expression profiling to identify differences in gene regulation between CRAMP-deficient and WT mice. As an exploratory tool, PCA of whole-genome expression profiles revealed that the effect of CRAMP deficiency created a sufficiently distinct gene expression profile compared to WT animals at baseline (Fig. 2a) and after CLP-induced sepsis (Fig. 2b) for further study. Analysis to identify differentially expressed genes showed that healthy animals (WT vs. CRAMP-deficient) did not differ in broad gene regulation pathways, but that CRAMP was markedly upregulated (22-fold) in WT septic animals (FDR *p* value = 5.17E−09, FC > 2), indicating that it is actively regulated during systemic infection and thus may have an active role in the response in mice.

To understand the distinct survival outcomes following CLP challenge, we compared the differentially expressed genes identified comparing septic vs. healthy CRAMP-deficient mice (1642 transcripts, FDR *p* value < 0.05, FC > 2) with the differentially expressed genes found comparing septic vs. healthy WT mice (1665 transcripts, FDR *p* value < 0.05, FC > 2) (Fig. 2c). A total of 1299 transcripts were regulated in a similar fashion between the two groups (Fig. 2d). Table 1 shows the functional annotation of 980 such genes, which includes clear activation of many broad immune response processes and inflammation-related pathways. In addition, the cytokine-cytokine receptor interaction pathway was particularly enriched (FDR *p* value 6.9E−10), with 49 genes regulated similarly in WT and CRAMP-deficient animals (*Cxcl1*, *Il1r2*, *Il1r1*, *Ccl3*, *Tnf*, *Ccl2*, *Il6st*, *Csf2rb2*, *Crlf2*, *Ccr1*, *Il18*, *Cxcl2*, *Il4ra*, *Ccl9*, *Cxcl9*, *Cxcr2*, *Ccl4*, *Ccl7*, *Cxcl10*, *Ccl24*, *Acvr1b*, *Tnfrsf1a*, *Cxcr5*, *Il1rap*, *Il1b*, *Fas*, *Il13ra1*, *Ifngr2*, *Ltb*, *Csf2ra*, *Lta*, *Il18rap*, *Ltbr*, *Met*, *Lifr*, *Tnfrsf13c*, *Tnfsf9*, *Osm*, *Inhba*, *Ccl12*, *Tnfrsf9*, *Ccr7*, *Ccr6*, *Ccr5*, *Il20rb*, *Ccr3*, *Cx3cr1*, *Ccr2*, and *Il5ra*).

In contrast to the large number of similarly regulated genes between septic and healthy animals in both groups, we found 79 genes that were significantly more expressed, and 119 that were significantly less expressed, when comparing the CLP sepsis response in CRAMP-deficient mice to their WT counterparts (FDR-corrected *p* value < 0.05, FC > 1.6). This smaller cohort of differentially expressed genes is likely to contain key immune response signatures underlying the robust phenotypic difference in mortality and changes in global gene expression (Figs. 1 and 2). Of note, *Camp* was the most upregulated gene (17-fold) in WT animals.

**Table 1** Gene Ontology (GO) analysis of genes similarly regulated between CRAMP-deficient and WT mice following systemic infection. Selected genes for this analysis showed FDR-corrected $p$ value <0.05 and a FC >2.0

| Term | Count | Gene symbol | FDR |
|---|---|---|---|
| GO:0006955 immune response | 92 | *ADORA3*, *CD8A*, *IL18*, *TIRAP*, *TLR2*, *PGLYRP1*, *TLR6*, *C1QC*, *CXCL10*, *CFP*, *C1RA*, *NOD2*, *MYD88*, *CLEC4E*, *IL1RAP*, *IL1B*, *FAS*, *CLEC4D*, *LBP*, *LTB*, *LTA*, *RAB27A*, *DAF2*, *CIITA*, *ICAM1*, *IL18RAP*, *H2-DMB1*, *H2-DMB2*, *CLEC4N*, *OSM*, *DCLRE1C*, *CCR7*, *H2-OA*, *CCR5*, *IL20RB*, *PSEN1*, *LAX1*, *SERPINA3G*, *CCR2*, *CX3CR1*, *LILRB4*, *H2-OB*, *H2-AA*, *CD300LF*, *CLEC5A*, *CXCL1*, *IL1F9*, *GPR183*, *IL1R1*, *CCL3*, *SBNO2*, *CCL2*, *TNF*, *C3*, *CXCL3*, *CXCL2*, *IL4RA*, *CCL9*, *CXCL9*, *PRKDC*, *OAS2*, *CCL4*, *CD74*, *CCL7*, *CCL24*, *RNF125*, *SLC11A1*, *GP49A*, *BCL3*, *PTX3*, *TCF3*, *DHX58*, *H60A*, *CR2*, *CFB*, *TLR13*, *IL1RN*, *TNFRSF13C*, *CTLA4*, *H2-AB1*, *TNFSF9*, *FCGR1*, *CD180*, *FCGR3*, *CCL12*, *CD55*, *FCGR2B*, *H2-EB1*, *C1RL*, *CD79B*, *CLEC7A*, *H2-DMA*, *CD14* | 6.74E−27 |
| GO:0006954 inflammatory response | 63 | *ADORA3*, *TLR2*, *TIRAP*, *TLR6*, *C1QC*, *CXCL10*, *CFP*, *C1RA*, *NOD2*, *MYD88*, *SAA1*, *IL1B*, *NOS2*, *LBP*, *LTA*, *DAF2*, *CIITA*, *NFKBIZ*, *SAA3*, *CD163*, *HIF1A*, *IL20RB*, *CCR5*, *CCR2*, *PLA2G7*, *KDM6B*, *CXCL1*, *CCL3*, *TNF*, *CCL2*, *C3*, *CCR1*, *CXCL3*, *CXCL2*, *CXCL9*, *CCL4*, *CCL7*, *TRF*, *CCL24*, *TNFRSF1A*, *SLC11A1*, *MEFV*, *PYCARD*, *FN1*, *CR2*, *CFB*, *SPHK1*, *ATRN*, *TLR13*, *FCGR1*, *CD180*, *STAT3*, *FCGR3*, *ORM1*, *CCL12*, *CD55*, *ITGB2L*, *NUPR1*, *STAB1*, *C1RL*, *CLEC7A*, *CD14*, *ORM2* | 2.27E−26 |
| GO:0002250 adaptive immune response | 24 | *ICAM1*, *CR2*, *CD8A*, *C3*, *CFB*, *IL18*, *TLR6*, *FCGR1*, *C1QC*, *CD74*, *FCGR3*, *SLC11A1*, *C1RA*, *CD55*, *NOD2*, *MYD88*, *FCGR2B*, *C1RL*, *H2-AA*, *BCL3*, *FAS*, *H2-DMA*, *DAF2*, *RAB27A* | 2.03E−08 |
| GO:0002526 acute inflammatory response | 23 | *CR2*, *ADORA3*, *C3*, *CFB*, *SAA3*, *C1QC*, *FCGR1*, *TRF*, *STAT3*, *CD163*, *FCGR3*, *CFP*, *ORM1*, *C1RA*, *CD55*, *NUPR1*, *SAA1*, *C1RL*, *IL1B*, *LBP*, *ORM2*, *DAF2*, *FN1* | 6.81E−08 |
| GO:0045087 innate immune response | 26 | *CIITA*, *IL1R1*, *IL18RAP*, *CR2*, *C3*, *CFB*, *TLR13*, *TLR2*, *TIRAP*, *TLR6*, *FCGR1*, *C1QC*, *CD180*, *CFP*, *SLC11A1*, *C1RA*, *CD55*, *NOD2*, *MYD88*, *IL1RAP*, *C1RL*, *LBP*, *CLEC7A*, *DHX58*, *DAF2*, *RAB27A* | 1.15E−07 |
| GO:0006935 chemotaxis | 26 | *C3AR1*, *CCL3*, *CCL2*, *CYSLTR1*, *S100A8*, *CXCL3*, *CCR1*, *CXCL2*, *S100A9*, *FPR1*, *CCL9*, *CXCR2*, *FPR2*, *CCL4*, *CCL7*, *CXCL10*, *CCL24*, *IL1B*, *LBP*, *C5AR1*, *FCGR3*, *PROK2*, *CCL12*, *CCR7*, *CCR3*, *CX3CR1* | 1.77E−07 |
| GO:0045321 leukocyte activation | 35 | *GPR183*, *SBNO2*, *ADORA3*, *CD8A*, *PRKDC*, *TPD52*, *CD74*, *SLC11A1*, *CXCR5*, *BCL11B*, *BCL11A*, *MS4A1*, *BCL3*, *FAS*, *LBP*, *TCF3*, *BLNK*, *RAB27A*, *EGR1*, *H60A*, *CR2*, *CRIP3*, *FCGR3*, *DCLRE1C*, *CARD11*, *BCL2A1D*, *CD86*, *PSEN1*, *FCGR2B*, *LAX1*, *CX3CR1*, *LCK*, *BANK1*, *H2-DMA*, *LCP2* | 5.97E−06 |
| GO:0001817 regulation of cytokine production | 26 | *TNF*, *ADORA2B*, *IL27RA*, *IL18*, *TLR2*, *TLR6*, *SLC11A1*, *IRAK3*, *NOD2*, *MYD88*, *HMOX1*, *PYCARD*, *IL1B*, *BCL3*, *LBP*, *LTB*, *H60A*, *CEBPB*, *SPHK1*, *TNFRSF13C*, *FCGR3*, *TIGIT*, *CARD11*, *IL20RB*, *CLEC7A*, *CD14* | 3.70E−05 |
| GO:0002478 antigen processing and presentation of exogenous peptide antigen | 11 | *H2-OA*, *FCGR2B*, *H2-EB1*, *H2-AA*, *H2-DMB1*, *H2-AB1*, *H2-DMA*, *FCGR1*, *CD74*, *H2-DMB2*, *FCGR3* | 1.02E−04 |
| GO:0002504 antigen processing and presentation of peptide or polysaccharide antigen via MHC class II | 10 | *H2-OA*, *FCGR2B*, *H2-OB*, *H2-EB1*, *H2-AA*, *H2-DMB1*, *H2-AB1*, *H2-DMA*, *CD74*, *H2-DMB2* | 1.92E−04 |
| GO:0009617 response to bacterium | 25 | *TNF*, *C5AR1*, *NGP*, *FGR*, *IL27RA*, *HCK*, *TIRAP*, *TLR2*, *PGLYRP1*, *NFKBIA*, *FCGR1*, *IRAK3*, *TNFRSF1A*, *SLC11A1*, *NOD2*, *MYD88*, *CCR5*, *STAB1*, *IL1B*, *BCL3*, *NOS2*, *LBP*, *TCF3*, *IRG1*, *CD14* | 0.001634157 |
| GO:0002764 ~ immune response-regulating signal transduction | 14 | *TLR2*, *NFKBIA*, *THY1*, *BCL2A1D*, *NOD2*, *MYD88*, *CD19*, *PSEN1*, *IL20RB*, *LAX1*, *LCK*, *SH2B2*, *CD79B*, *CLEC7A* | 0.0019905 |
| GO:0060627 regulation of vesicle-mediated transport | 17 | *SEPT5*, *ADORA3*, *ADORA2B*, *C3*, *CD63*, *SIRPA*, *FCGR1*, *FCGR3*, *SLC11A1*, *MIB1*, *NOD2*, *FCGR2B*, *PRAM1*, *HMOX1*, *RAPGEF4*, *CLEC7A*, *PTX3* | 0.005043353 |
| GO:0045807 positive regulation of endocytosis | 11 | *MIB1*, *SLC11A1*, *NOD2*, *FCGR2B*, *C3*, *CLEC7A*, *PTX3*, *CD63*, *SIRPA*, *FCGR1*, *FCGR3* | 0.007062817 |

When upregulated genes in septic CRAMP-deficient mice were compared with septic WT mice, other differences including sepsis markers were emphasized (Table 2). CD14, a pattern recognition receptor of the innate immune response that facilitates presentation of bacterial components to Toll-like receptors, was highly upregulated in septic animals, but the upregulation was more intense in CRAMP-deficient mice vs. WT controls, a finding we confirmed by qPCR (Supplementary

Fig. 1). Other genes associated with bacterial responses and presenting with the same regulation pattern were *Il-1β*, *Slc11a1*, *C5ar1*, *Lbp*, and *Irg1* (GO:0002237 term: response to molecule of bacterial origin, FDR *p* value 0.001). A similar regulation of 11 genes associated with chemotaxis and/or leukocyte migration *Prok2*, *C5ar1*, *S100a8*, *CysLT1*, *Ccr1*, *S100a9*, *Fpr1*, *Il-1β*, *Cxcr2*, *Lbp*, and *Fcgr3* (Table 2) (GO:0006935 term: chemotaxis, FDR *p* value 1.5E−06) was also identified. Taken together, these differences indicate that aspects of the innate immune response to CLP challenge are more robust in CRAMP-deficient mice. Indeed, we found increased plasma levels of IL-1β, IL-6, and the mouse chemoattractant peptide-1 (MCP-1) in CRAMP-deficient mice compared to WT animals (Fig. 3), confirming that cathelicidin deficiency can be associated with compensatory increases in other inflammatory response pathways in this mouse model. No significant differences were noted in serum-level tumor necrosis factor-α or anti-inflammatory cytokine IL-10 following CLP in CRAMP-deficient vs. WT mice.

We explored phenotypic correlates of the changes in immune gene and cytokine expression. No difference was observed between CRAMP-deficient and WT mice in phagocytosis of *E. coli* bacteria (Fig. 4a). However, when the number of cells in the peritoneum of septic animals was enumerated, we found a significant increase in neutrophils in the peritoneal cavity of CRAMP-deficient mice compared with WT animals (Fig. 4b), indicating possible differences in chemotaxis. Moreover, the percentage of apoptotic cells in the peritoneal cavity of CRAMP-deficient mice was lower than that of WT mice (Fig. 4c), and greater immune cell resilience in the face of the CLP-induced sepsis may promote cytokine expression and resistance to mortality.

## Discussion

Multiresistant bacteria are an ongoing problem that complicates sepsis therapy, and antibiotics that act to lyse bacterial membranes may increase the liberation of pro-inflammatory cell components, possibly augmenting the severity of the inflammatory response. Because AMPs seem not only to kill bacteria but to neutralize pathogenic factors and regulate the immune response, they are considered potential therapeutic options for treating severe infections [27]. However, their mechanisms of action, side effects, and specific outcomes are likely to depend on the disease type and have not been completely elucidated. Despite that, cathelicidin administration has been proposed as a potential antisepsis therapeutic based on its LPS-binding properties and direct antimicrobial activities [28].

Our group has shown that LL-37, the human cathelicidin, is downregulated in septic shock and others have shown that LL-37 is downregulated in sepsis [23, 24]. We have also previously shown that LPS- and flagellin-mediated inflammatory responses are potentiated in vitro by cathelicidin [29]. Based on these results, we proposed that LL-37 administration may have unpredictable effects on the systemic inflammatory response to severe infection and must be approached with caution [23]. In the current study, we show that CRAMP-deficient mice experienced better survival following CLP in association

**Table 2** Differentially expressed genes between CRAMP-deficient septic mice (KS) and matched healthy animals (KH) and between septic WT animals (WS) and matched healthy controls (WH)

| Gene symbol | *p* (corr) | FC (KH vs. KS) | FC (WH vs. WS) | FC (K vs. W) | Description |
|---|---|---|---|---|---|
| *Cd14* | 9.89E−16 | −176.89 | −98.55 | 1.79 | *Mus musculus* CD14 antigen (CD14) |
| *Il1b* | 5.14E−07 | −7.96 | −4.23 | 1.88 | *Mus musculus* interleukin 1 beta (IL-1b) |
| *Slc11a1* | 3.74E−06 | −7.36 | −4.10 | 1.80 | *Mus musculus* solute carrier family 11 |
| *C5ar1* | 9.66E−05 | −10.21 | −3.33 | 3.07 | *Mus musculus* complement component 5a receptor 1 (C5ar1) |
| *Lbp* | 7.65E−07 | −29.33 | −12.90 | 2.27 | *Mus musculus* lipopolysaccharide-binding protein (Lbp) |
| *Irg1* | 2.68E−10 | −121.10 | −35.93 | 3.37 | *Mus musculus* immunoresponsive gene 1 (Irg1) |
| *Prok2* | 1.64E−09 | −38.93 | −15.74 | 2.47 | *Mus musculus* prokineticin 2 (Prok2) |
| *S100a8* | 1.65E−09 | −12.40 | −5.60 | 2.22 | *Mus musculus* S100 calcium-binding protein A8 (calgranulin A) (S100a8) |
| *Cysltr1* | 0.001 | −4.56 | −2.44 | 1.87 | *Mus musculus* cysteinyl leukotriene receptor 1 (Cysltr1) |
| *Ccr1* | 1.31E−08 | −14.90 | −9.29 | 1.60 | *Mus musculus* chemokine (C-C motif) receptor 1 (Ccr1) |
| *S100a9* | 2.54E−08 | −8.55 | −4.22 | 2.02 | *Mus musculus* S100 calcium-binding protein A9 (calgranulin B) (S100a9) |
| *Fpr1* | 1.52E−11 | −14.24 | −8.41 | 1.69 | *Mus musculus* formyl peptide receptor 1 (Fpr1) |
| *Cxcr2* | 3.22E−05 | −5.42 | −2.41 | 2.25 | *Mus musculus* chemokine (C-X-C motif) receptor 2 (Cxcr2) |
| *Fcgr3* | 2.42E−06 | −7.02 | −4.22 | 1.66 | *Mus musculus* Fc receptor, IgG, low affinity III (Fcgr3) |

Negative numbers indicate upregulation in septic animals. K: (KH vs. KS); W: (WH vs. WS)

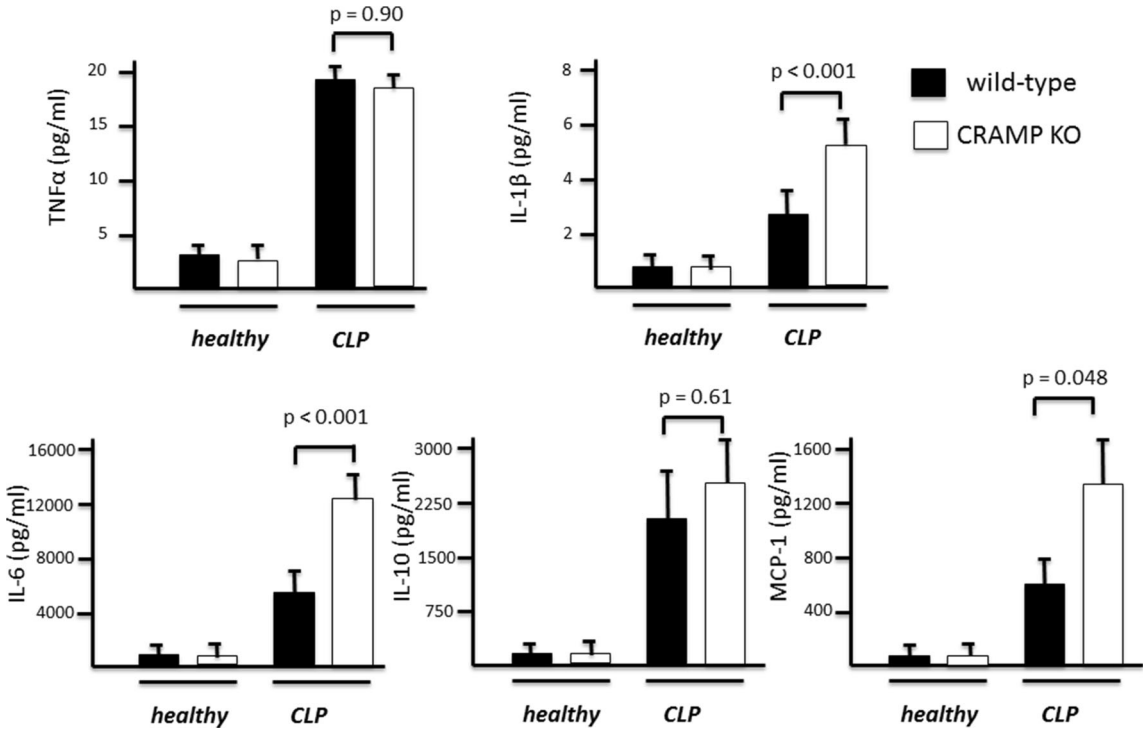


**Fig. 3** Cytokine levels. TNFα, IL-1β, IL-6, IL-10, and MCP-1 plasma levels in healthy WT and CRAMP-deficient mice 8 h after CLP ($n = 8$ animals per group)

with increased levels of key pro-inflammatory cytokines of the innate immune response. It is well established that the endotoxemia in the model of CLP, which is considered to model peritonitis associated with ruptured appendix or gastrointestinal surgery, is lower than that produced by models of direct injection of LPS or live *E. coli* [30].

Consistent with our results, Danka et al. observed that CRAMP-deficient mice were more resistant to *E. coli* cystitis [31] and suggested that this difference was based on the cathelicidin-induced increase of local inflammation. On the other hand, Chromek et al. found that CRAMP protected mice from enteric infection of the gastrointestinal tract with *E. coli* O157:H7 [32]. Since several bacteria, including *E. coli*, have developed resistance and evasion mechanisms to cathelicidins and other AMPs [33–35], we believe that many different pathologic scenarios are possible, depending on the strain and challenge model involved, in particular comparing mucosal to systemic infection.

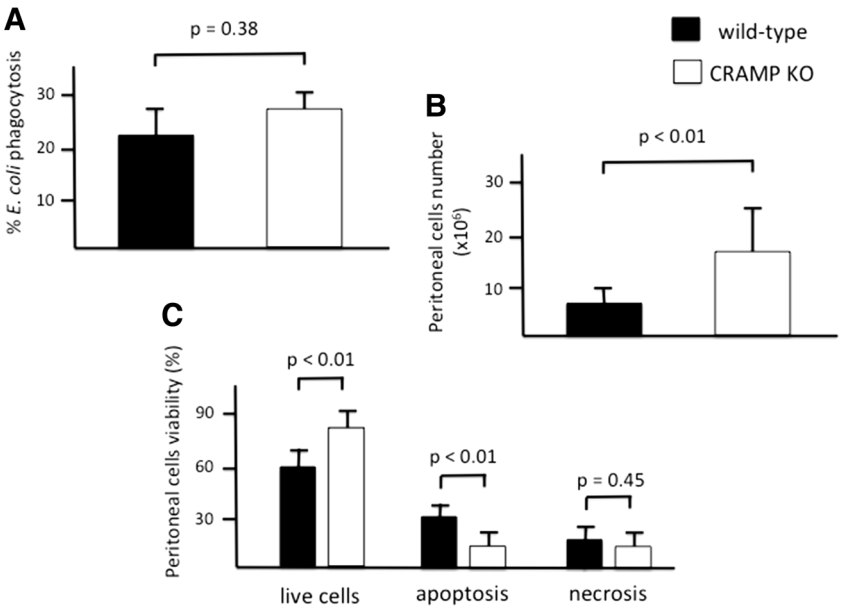


**Fig. 4** **a** Phagocytosis assay. *E. coli* was incubated with peritoneal macrophages from CRAMP-deficient and WT mice and phagocytosis was assessed by flow cytometry. **b** Neutrophil recruitment assay. Neutrophils were obtained from CRAMP-deficient ($n = 5$) and WT ($n = 8$) mice by peritoneal lavage 24 h after CLP and the number of cells was counted. **c** Apoptosis assay. Cell viability of neutrophils from the peritoneal cavity of CRAMP-deficient and WT mice was assessed by flow cytometry. All experiments were performed in triplicate

Cirioni et al. [36] and Beaumont et al. [37] studied the role of intravenously administered human cathelicidin on sepsis in rats and pulmonary infection in mice, respectively, observing potential beneficial therapeutic effects. Methodological differences between this study and our present work include pharmacological application of the human cathelicidin (LL-37) compared to our work which studies endogenous deficiency of the cathelicidin of the experimental animal species. Cathelicidins from different species (rats and mice produce CRAMP) diverge in many biological activities [38], and exogenous administration at supraphysiologic dosage could be associated with cytotoxicity or effects on cell signaling, generating contrasting results [39].

Global gene expression analyses suggested that differences in mortality between septic CRAMP-deficient mice and septic WT mice could be related to immunomodulatory properties of CRAMP or its effect on immune cell death regulation, considering distinct levels of cytokine and chemokine gene expression, neutrophil recruitment, and differential expression of CD14, a key LPS receptor.

The phagocytic capacity of macrophages was evaluated in vitro between WT and CRAMP-deficient mice and differences were not statistically significant (Fig. 4a). Some authors have shown that LL-37 induces phagocytosis [40]. CD14-dependent phagocytosis by mononuclear phagocytes has been demonstrated for several bacteria [41–43] and also for apoptotic cells [44]. Our assay, however, was not able to demonstrate that macrophages from CRAMP-deficient mice, with higher CD14 expression, had higher phagocytic capacity when stimulated in vitro, but further investigations are necessary to address this question in other biological conditions.

In the context of CLP-induced sepsis, and in agreement with gene expression results, plasma levels of the pro-inflammatory cytokines IL-1β and IL-6 were higher in CRAMP-deficient mice, while TNFα and IL-10 did not differ significantly from WT animals (Fig. 3). Chemokines are critical in the immune response to infection, and MCP-1 was higher in septic CRAMP-deficient mice (Fig. 3), paralleling a higher number of neutrophils in the peritoneal cavity (Fig. 4b). Taken together, these results presented in a C57BL/6 background may contribute to the understanding of the enhanced survival potential of CRAMP-deficient mice following CLP and support an immunomodulatory, and in some cases anti-inflammatory, profile associated with *Camp* expression. CRAMP binding to LPS to diminish its signaling potential or increased apoptotic macrophage cell death in WT vs. CRAMP-deficient mice could contribute to impaired inflammatory response and increased mortality in the CLP model.

Cathelicidins may have multiple mechanisms of action, not only at the cell membrane but also in the cytoplasm [45] and at the nuclear level [46, 47]. The full repertoire of mechanisms of action of cathelicidins remains to be defined, even though their dualistic function (inflammatory and anti-inflammatory), depending on the disease and cellular context, is becoming manifest. The comprehension of this dual role is essential for potential clinical applications, and our work contributes to this knowledge.

## Conclusion

In this study, we demonstrated that CRAMP-deficient mice with systemic infection showed increased survival, which was associated with an upregulation of certain key genes related to immune response and increased neutrophil infiltration to the site of infection. Further studies are necessary to investigate the role of cathelicidins in sepsis caused by different pathogenic bacterial strains, to clarify their multifarious roles in the response to systemic infection.

**Acknowledgements** FPS is supported by FAPESP, the São Paulo Research Foundation (grant no. 2015/00892-4).

**Compliance with ethical standards** All experiments were performed when animals were 8–12 weeks old and protocols followed in accordance with the University of São Paulo Faculty of Medicine Animal Facility guidelines through protocols approved by their ethics committee.

**Conflict of interest** The authors declare that they have no conflict of interest.

## References

1. Zaiou M, Gallo RL (2002) Cathelicidins, essential gene-encoded mammalian antibiotics. J Mol Med (Berl) 80:549–561
2. Ramanathan B, Davis EG, Ross CR, Blecha F (2002) Cathelicidins: microbicidal activity, mechanisms of action, and roles in innate immunity. Microbes Infect 4:361–372
3. Durr UH, Sudheendra US, Ramamoorthy A (2006) LL-37, the only human member of the cathelicidin family of antimicrobial peptides. Biochim Biophys Acta 1758:1408–1425
4. Gallo RL, Kim KJ, Bernfield M, Kozak CA, Zanetti M, Merluzzi L, Gennaro R (1997) Identification of CRAMP, a cathelin-related antimicrobial peptide expressed in the embryonic and adult mouse. J Biol Chem 272:13088–13093
5. Gudmundsson GH, Agerberth B, Odeberg J, Bergman T, Olsson B, Salcedo R (1996) The human gene FALL39 and processing of the cathelin precursor to the antibacterial peptide LL-37 in granulocytes. Eur J Biochem 238:325–332
6. Pinheiro da Silva F, Machado MC (2012) Antimicrobial peptides: clinical relevance and therapeutic implications. Peptides 36:308–314
7. Nizet V, Ohtake T, Lauth X, Trowbridge J, Rudisill J, Dorschner RA, Pestonjamasp V, Piraino J, Huttner K, Gallo RL (2001) Innate antimicrobial peptide protects the skin from invasive bacterial infection. Nature 414:454–457
8. Iimura M, Gallo RL, Hase K, Miyamoto Y, Eckmann L, Kagnoff MF (2005) Cathelicidin mediates innate intestinal defense against colonization with epithelial adherent bacterial pathogens. J Immunol 174:4901–4907
9. Chromek M, Slamova Z, Bergman P, Kovacs L, Podracka L, Ehren I, Hokfelt T, Gudmundsson GH, Gallo RL, Agerberth B et al (2006) The antimicrobial peptide cathelicidin protects the urinary tract against invasive bacterial infection. Nat Med 12:636–641

10. Huang LC, Jean D, Proske RJ, Reins RY, McDermott AM (2007) Ocular surface expression and in vitro activity of antimicrobial peptides. Curr Eye Res 32:595–609
11. Oren Z, Lerman JC, Gudmundsson GH, Agerberth B, Shai Y (1999) Structure and organization of the human antimicrobial peptide LL-37 in phospholipid membranes: relevance to the molecular basis for its non-cell-selective activity. Biochem J 341(Pt 3):501–513
12. Ciornei CD, Sigurdardottir T, Schmidtchen A, Bodelsson M (2005) Antimicrobial and chemoattractant activity, lipopolysaccharide neutralization, cytotoxicity, and inhibition by serum of analogs of human cathelicidin LL-37. Antimicrob Agents Chemother 49:2845–2850
13. Larrick JW, Hirata M, Balint RF, Lee J, Zhong J, Wright SC (1995) Human CAP18: a novel antimicrobial lipopolysaccharide-binding protein. Infect Immun 63:1291–1297
14. Ries M, Schuster P, Thomann S, Donhauser N, Vollmer J, Schmidt B (2013) Identification of novel oligonucleotides from mitochondrial DNA that spontaneously induce plasmacytoid dendritic cell activation. J Leukoc Biol 94:123–135
15. Wewers MD, Sarkar A (2009) P2X(7) receptor and macrophage function. Purinergic Signal 5:189–195
16. Coffelt SB, Tomchuck SL, Zwezdaryk KJ, Danka ES, Scandurro AB (2009) Leucine leucine-37 uses formyl peptide receptor-like 1 to activate signal transduction pathways, stimulate oncogenic gene expression, and enhance the invasiveness of ovarian cancer cells. Mol Cancer Res 7:907–915
17. Yin J, Yu FS (2010) LL-37 via EGFR transactivation to promote high glucose-attenuated epithelial wound healing in organ-cultured corneas. Invest Ophthalmol Vis Sci 51:1891–1897
18. Tjabringa GS, Ninaber DK, Drijfhout JW, Rabe KF, Hiemstra PS (2006) Human cathelicidin LL-37 is a chemoattractant for eosinophils and neutrophils that acts via formyl-peptide receptors. Int Arch Allergy Immunol 140:103–112
19. Niyonsaba F, Iwabuchi K, Someya A, Hirata M, Matsuda H, Ogawa H, Nagaoka I (2002) A cathelicidin family of human antibacterial peptide LL-37 induces mast cell chemotaxis. Immunology 106:20–26
20. Salzer S, Kresse S, Hirai Y, Koglin S, Reinholz M, Ruzicka T, Schauber J (2014) Cathelicidin peptide LL-37 increases UVB-triggered inflammasome activation: possible implications for rosacea. J Dermatol Sci 76:173–179
21. Nagaoka I, Suzuki K, Niyonsaba F, Tamura H, Hirata M (2012) Modulation of neutrophil apoptosis by antimicrobial peptides. ISRN Microbiol 2012:345791
22. von Kockritz-Blickwede M, Goldmann O, Thulin P, Heinemann K, Norrby-Teglund A, Rohde M, Medina E (2008) Phagocytosis-independent antimicrobial activity of mast cells by means of extracellular trap formation. Blood 111:3070–3080
23. Barbeiro DF, Barbeiro HV, Zampieri FG, Cesar Machado MC, Torggler Filho F, Gomes Cunha DM, Goulart AC, Velasco IT, Monteiro da Cruz Neto L, Possolo de Souza H et al (2013) Cathelicidin LL-37 bloodstream surveillance is down regulated during septic shock. Microbes Infect 15:342–346
24. Jeng L, Yamshchikov AV, Judd SE, Blumberg HM, Martin GS, Ziegler TR, Tangpricha V (2009) Alterations in vitamin D status and anti-microbial peptide levels in patients in the intensive care unit with sepsis. J Transl Med 7:28
25. Wichterman KA, Baue AE, Chaudry IH (1980) Sepsis and septic shock–a review of laboratory models and a proposal. J Surg Res 29: 189–201
26. Livak KJ, Schmittgen TD (2001) Analysis of relative gene expression data using real-time quantitative PCR and the 2(-Delta Delta C(T)) Method. Methods 25:402–408
27. Martin L, van Meegern A, Doemming S, Schuerholz T (2015) Antimicrobial Peptides in Human Sepsis. Front Immunol 6:404
28. Mookherjee N, Rehaume LM, Hancock RE (2007) Cathelicidins and functional analogues as antisepsis molecules. Expert Opin Ther Targets 11:993–1004
29. Pinheiro da Silva F, Gallo RL, Nizet V (2009) Differing effects of exogenous or endogenous cathelicidin on macrophage toll-like receptor signaling. Immunol Cell Biol 87(6):496–500
30. Kingsley SM, Bhat BV (2016) Differential Paradigms in Animal Models of Sepsis. Curr Infect Dis Rep 18:26
31. Danka ES, Hunstad DA (2015) Cathelicidin augments epithelial receptivity and pathogenesis in experimental Escherichia coli cystitis. J Infect Dis 211:1164–1173
32. Chromek M, Arvidsson I, Karpman D (2012) The antimicrobial peptide cathelicidin protects mice from Escherichia coli O157:H7-mediated disease. PLoS One 7:e46476
33. Audrain B, Ferrieres L, Zairi A, Soubigou G, Dobson C, Coppee JY, Beloin C, Ghigo JM (2013) Induction of the Cpx envelope stress pathway contributes to Escherichia coli tolerance to antimicrobial peptides. Appl Environ Microbiol 79:7770–7779
34. Cole JN, Nizet V (2016) Bacterial evasion of host antimicrobial peptide defenses. Microbiol Spectr 4. doi:10.1128/microbiolspec.VMBF-0006-2015
35. Thomassin JL, Brannon JR, Kaiser J, Gruenheid S, Le Moual H (2012) Enterohemorrhagic and enteropathogenic Escherichia coli evolved different strategies to resist antimicrobial peptides. Gut Microbes 3:556–561
36. Cirioni O, Giacometti A, Ghiselli R, Bergnach C, Orlando F, Silvestri C, Mocchegiani F, Licci A, Skerlavaj B, Rocchi M et al (2006) LL-37 protects rats against lethal sepsis caused by gram-negative bacteria. Antimicrob Agents Chemother 50:1672–1679
37. Beaumont PE, McHugh B, Gwyer Findlay E, Mackellar A, Mackenzie KJ, Gallo RL, Govan JR, Simpson AJ, Davidson DJ (2014) Cathelicidin host defence peptide augments clearance of pulmonary Pseudomonas aeruginosa infection by its influence on neutrophil function in vivo. PLoS One 9:e99029
38. Coorens M, Scheenstra MR, Veldhuizen EJ, Haagsman HP (2017) Interspecies cathelicidin comparison reveals divergence in antimicrobial activity, TLR modulation, chemokine induction and regulation of phagocytosis. Sci Rep 7:40874
39. Pinheiro da Silva F, Machado MC (2017) The dual role of cathelicidins in systemic inflammation. Immunol Lett 182:57–60
40. Wan M, van der Does AM, Tang X, Lindbom L, Agerberth B, Haeggstrom JZ (2014) Antimicrobial peptide LL-37 promotes bacterial phagocytosis by human macrophages. J Leukoc Biol 95:971–981
41. Peterson PK, Gekker G, Hu S, Sheng WS, Anderson WR, Ulevitch RJ, Tobias PS, Gustafson KV, Molitor TW, Chao CC (1995) CD14 receptor-mediated uptake of nonopsonized Mycobacterium tuberculosis by human microglia. Infect Immun 63:1598–1602
42. Muro M, Koseki T, Akifusa S, Kato S, Kowashi Y, Ohsaki Y, Yamato K, Nishijima M, Nishihara T (1997) Role of CD14 molecules in internalization of Actinobacillus actinomycetemcomitans by macrophages and subsequent induction of apoptosis. Infect Immun 65:1147–1151
43. Lipovsky MM, Gekker G, Anderson WR, Molitor TW, Peterson PK, Hoepelman AI (1997) Phagocytosis of nonopsonized Cryptococcus neoformans by swine microglia involves CD14 receptors. Clin Immunol Immunopathol 84:208–211
44. Devitt A, Moffatt OD, Raykundalia C, Capra JD, Simmons DL, Gregory CD (1998) Human CD14 mediates recognition and phagocytosis of apoptotic cells. Nature 392:505–509
45. Nakagawa Y, Gallo RL (2015) Endogenous intracellular cathelicidin enhances TLR9 activation in dendritic cells and macrophages. J Immunol 194:1274–1284
46. Pinheiro da Silva F, Medeiros MC, Dos Santos AB, Ferreira MA, Garippo AL, Chammas R, Caldini E, Velasco IT, Possolo de Souza H, Machado MC (2013) Neutrophils LL-37 migrate to the nucleus during overwhelming infection. Tissue Cell 45:318–320
47. Munoz M, Craske M, Severino P, de Lima TM, Labhart P, Chammas R, Velasco IT, Machado MC, Egan B, Nakaya HI et al (2016) Antimicrobial peptide LL-37 participates in the transcriptional regulation of melanoma cells. J Cancer 7:2341–2345